Fourth International Symposium on Marine Propulsors
smp'15, Austin, Texas, USA, June 2015

An Extrapolation Method Suitable for Scaling of Propellers of any Design

Dr. Stephan Helma[1]

[1] Stone Marine Propulsion Ltd
Dock Road, Birkenhead, Merseyside, CH41 1DT, United Kingdom

ABSTRACT

The extrapolation procedures currently used to scale propeller characteristics tested at model scale to their full scale performances are either based on a statistical, the Lerbs-Meyne or the recently developed strip method.

With the emergence of so-called unconventional propellers and different design strategies associated with them, it has been questioned whether the assumptions used in these scaling methods are still universally valid. E.g. with tip and root unloading employed the circulation distribution deviates from the optimum, which is assumed by the Lerbs-Meyne method; more modern profiles show a different camber distribution and hence the drag coefficient must be aligned with the hydrodynamic inflow angle and not with the pitch to diameter ratio as assumed by the strip method (and implicitly by the ITTC 1978 method).

The work presented still uses the assumption of the equivalent profile and will explain three possible modified scaling procedures ultimately resulting in a way to calculate the hydrodynamic inflow angle solely from one open-water test conducted at a constant Reynolds number. Finally exemplary results comparing a propeller of conventional type with a recent propeller designs will also be shown.

The new proposed method shows a superior performance when compared to other scaling methods.

Keywords

Scale effects, ITTC 1978 power prediction, Lerbs-Meyne, Strip method, Open-water efficiency.

1 INTRODUCTION

In recent years, new propeller design philosophies have emerged into the market. The NPT-, Kappel- and CLT-propellers are examples of these so-called unconventional designs. From the very beginning it was claimed by their designers that the existing scaling methods do not result in full scale predictions reflecting the actual performances observed. Based on the data available to the author this holds true for at least one of the above mentioned propeller types: The trial results regularly show a performance above the speeds predicted by different model basins. Generally speaking this behavior never posed a problem in the past. With everybody now looking for the most efficient configuration more and more propellers are comparatively tested and the final design is decided on the outcome of the performance predictions. Some propeller manufactures even take the scaling procedure used at the model basin into their consideration when designing a propeller for a comparative test to gain a little advantage over competitors. These tests pose a complete new challenge to the model basins, since tiny differences – often as small as 0.01 kn – determine who wins the contract. This shows clearly that a more accurate scaling procedure is in high demand.

A "good" procedure to extrapolate open-water data measured in a towing tank to full scale data must satisfy the following criteria to be reliable and trustworthy:

1. Independence on the Reynolds number of the model test:
   The extrapolated performance must be independent of the Reynolds number of the open-water data, which means, that regardless of the Reynolds number experienced during the model test, the full scale prediction must be the same.
2. Independence of the propeller geometry:
   The extrapolated performance must reproduce the relative merits of different propeller designs, that the same procedure can be used for any design and no design should be favored.
3. Absolute accuracy:
   The extrapolated performance must represent the actual performance figures of the propeller, although a predictable difference can be handled with an adjustment factor.
4. Reliability:
   The analysis of the open-water data must give a criteria about the reliability of the test.

2 EXISTING SCALING PROCEDURES

Currently four main scaling procedures are used in model basins to scale the measured open-water data to full scale propeller performance:

1. No scaling

2. ITTC 1978 extrapolation method
3. Lerbs-Meyne method
4. Strip method

Independently of the scaling method applied, there are some local preferences in the implementation of the open-water tests, mainly concerning the Reynolds number used. Some model basins adheres strictly to the ITTC recommendation that the Reynolds number "must not be lower than $2 \cdot 10^5$ at the open-water test" (ITTC 1999) (some of them just fulfilling the recommendation running the open-water test at a Reynolds number of $2 \cdot 10^5$); some model basins conduct two tests (one at the Reynolds number experienced during the self-propulsion test and one above $2 \cdot 10^5$, using the lower to analyze the self-propulsion test, the other to scale to the full scale open-water curve); at least one model basin arranges for three open-water tests (one at the Reynolds number of the self-propulsion and two higher ones "to assess if the flow is fully turbulent"). If just one open-water test is conducted, it might or might not be scaled down to the Reynolds number experienced at the self-propulsion test.

2.1 No Scaling

When prediction the full scale performance, the open-water test is not extrapolated to full scale, but a final correction factor is applied to the performance prediction.

2.2 ITTC 1978 Extrapolation Method

The ITTC 1978 extrapolation method assumes a linear correlation between the change in friction drag and change in thrust and torque coefficient (ITTC 1999). But "it should be kept in mind that both the relation between thrust/torque and drag coefficient and the relation between drag coefficient and Reynolds number are based on statistics and the basis for the statistical values is very small" (Kuiper 1992). This very clear warning should always be kept in mind when judging the accuracy of any results using this extrapolation method. With the emergence of new profile types this warning becomes more and more vehemently – especially when comparing propellers using different profile types.

The second problematic characteristics of this scaling method is the linear dependence of the change in the thrust coefficient on the pitch to diameter ratio P/D. To explain the impact of this assumption, let us consider a propeller with a flat camber line and compare it to one, where all the lift is generated by camber alone. The first propeller will have a higher pitch because the lift is only generated by the angle of incidence. Even if this propeller will perform worse than the cambered one, it will be favored by the extrapolation method and might show a scaled performance superior to the second, cambered propeller.

The ITTC 1978 extrapolation method insists to test the propeller model at a Reynolds number "not […] lower than $2 \cdot 10^5$ at the open-water test" (ITTC 1999). If you compared the performance extrapolated from open-water tests conducted at different Reynolds numbers you want to get the same values independently from the starting point. Figure 2 shows three full scale open-water curves of the same propeller but scaled up from different Reynolds numbers according to ITTC. Evidently the curve calculated from the lowest Reynolds number does not coincide with the other two curves despite the fact that the lowest Reynolds number of about $2.5 \cdot 10^5$ is well above the ITTC 1978 recommendation of $2 \cdot 10^5$. The propeller shown in figure 7 exhibits an even worse behavior: There is a big difference in the extrapolated performances depending on the starting point. The first propeller tested was of a Wageningen B type, the second was of the NPT type. Both propellers were tested at the same model basin.

2.3 Lerbs-Meyne-Method

The Lerbs-Meyne method was published in 1968 (Moyne 1968) and derives a propeller with optimum distribution of circulation and no friction, that is the ideal propeller, from the open-water test at one Reynolds number. With an assumed drag ratio $\varepsilon_{0.7}$ of the so called equivalent profile at radius $0.7R$, the measured values η and c_{TH}, the open-water efficiency and the thrust coefficient, respectively, can be converted to η_i and c_{THi} of the ideal propeller. However there is only one valid combination of η_i and c_{THi} which can be read of the Kramer diagram (1939). Most likely the calculated $\eta_i(\varepsilon_{0.7})$ and $c_{THi}(\varepsilon_{0.7})$ do not coincide with the valid combination, so $\varepsilon_{0.7}$ has to be adjusted in an iterative process until the valid combination is met. The full scale values are calculated with a friction coefficient of 0.006.

The Lerbs-Meyne method seems to be the perfect scaling method, since the profile drag is calculated from the actually measured open-water values and it is aligned with the inflow. There are only two drawbacks. Firstly, it is based on an equivalent profile which represents the whole propeller blade. Secondly, it assumes that the propeller blade was designed with an optimum circulation distribution. This poses a problem with modern propellers which are almost always wake adapted designs. The designer also often unloads the tip or root region or the diameter is restricted, so the assumption of optimum circulation distribution does not hold for all designs.

The figures 3 and 8 show the scaled open-water tests.

2.4 Strip method

The strip method was developed by H. Streckwall of the HSVA model basin and published in 2013 (Streckwall et al

2013). When analyzing an open-water test, the vector sum of the contributions of each radial section (strip) towards the friction resistance is calculated to get the friction resistance of the whole blade. When doing so, it takes into account the actual Reynolds number and the position of the transition point at the respective radial strip.

The strip method is certainly an advancement of the existing scale methods. The advantages are that it accounts for the actual turbulence in the inflow, e.g. in open-water and behind condition, by using two different friction lines. It also takes into account the actual distribution of chord length and pitch. The main potential problems are the alignment of the drag forces with the nose-tail pitch line instead of the actual inflow angle (see the respective note in section 2.2 about the ITTC 1978 extrapolation procedure) and the determination of the friction coefficients. As pointed out by Streckwall the calculation of the friction coefficient uses the local friction coefficients for laminar and turbulent flow as stated by Hoerner (1965) and the location of the transition point is derived from CFD calculations. These calculations were done for a set of propellers for two inflow conditions: One with low turbulence for the open-water curve, one with higher turbulence for the behind condition as expected during self-propulsion tests. Final curve fittings result in the two friction resistance curves for the open-water and the behind condition. These derived curves are used for all propellers disregarding the actual profile used, whereas it is to be expected that the location of the transition point is strongly influenced by the section shape.

The scaled open-water tests can be found in figures 4 and 9.

3 NEW SCALING METHODS, THREE OPTIONS

In the author's opinion the second goal of independence of the propeller geometry can only be realized if the drag coefficient is not parallel to the nose-tail pitch line but aligned with the hydrodynamic inflow as the theory of thin profiles suggests. Three ways to derive the hydrodynamic inflow angle from open-water tests will be shown in the following sections.

3.1 Equivalent Profile

Let us imagine that the propeller is built up of circumferential sections stacked on top of each other and each section experiences a lift and drag coefficient c_d and c_l. These coefficients are aligned with the hydrodynamic inflow angle β_i. Geometric considerations lead to the formulae (1a+b) for the thrust and torque coefficients K_T and K_Q:

$$K_T = \frac{\pi^2 Z}{4}\int_{x_h}^{1} \frac{c_l(x)\cos\beta_i(x) - c_d(x)\sin\beta_i(x)}{\left[\frac{\cos\beta(x)}{\cos(\beta_i(x)-\beta(x))}\right]^2}\frac{c(x)}{D}x^2\mathrm{d}x \tag{1a}$$

$$K_Q = \frac{\pi^2 Z}{8}\int_{x_h}^{1} \frac{c_l(x)\sin\beta_i(x) + c_d(x)\cos\beta_i(x)}{\left[\frac{\cos\beta(x)}{\cos(\beta_i(x)-\beta(x))}\right]^2}\frac{c(x)}{D}x^3\mathrm{d}x \tag{1b}$$

where

Z = the number of propeller blades,

x = the fractional radius r/R,

x_h = the fractional radius r_h/R of the propeller hub,

$c(x)$ = the length of the section at fractional radius x,

$\beta(x)$ = the advance angle at fractional radius x,

$\beta_i(x)$ = the hydrodynamic inflow angle and

D = the propeller diameter.

At this point we introduce the concept of the equivalent profile: We replace the whole propeller blade with one single section of length $\overline{c}$ located at the fractional radius $\overline{x}$ such that this profile shows the same characteristics as the original blade. Using this equivalent profile we can replace the chord distribution and all hydrodynamic values which depend on the fractional radius x in the integrand with constant values and extract these from the integral. We denote these values of the equivalent profile with the overbar $\overline{\ }$:

$$K_T = \frac{\pi^2 Z}{4}\frac{\overline{c}_l\cos\overline{\beta}_i - \overline{c}_d\sin\overline{\beta}_i}{\left[\frac{\cos\overline{\beta}}{\cos(\overline{\beta}_i-\overline{\beta})}\right]^2}\frac{\overline{c}}{D}\int_{x_h}^{1} x^2\mathrm{d}x \tag{2a}$$

$$K_Q = \frac{\pi^2 Z}{8}\frac{\overline{c}_l\cos\overline{\beta}_i + \overline{c}_d\sin\overline{\beta}_i}{\left[\frac{\cos\overline{\beta}}{\cos(\overline{\beta}_i-\overline{\beta})}\right]^2}\frac{\overline{c}}{D}\int_{x_h}^{1} x^3\mathrm{d}x \tag{2b}$$

(For an alternative formulation of the equivalent profile, see appendix “A.1 Alternative Formulation of the Equivalent Profile”.)

Note that for the equivalent profile the thrust and torque coefficients must remain the same as for the whole propeller blade, hence the $\overline{\ }$ can be omitted.

After integration the equations (2a+b) become:

$$K_T = \frac{\pi^2 Z}{4}\frac{\overline{c}_l\cos\overline{\beta}_i - \overline{c}_d\sin\overline{\beta}_i}{\left[\frac{\cos\overline{\beta}}{\cos(\overline{\beta}_i-\overline{\beta})}\right]^2}\frac{\overline{c}}{D}\frac{1-x_h^3}{3} \tag{3a}$$

$$K_Q = \frac{\pi^2 Z}{8} \frac{\bar{c}_l \sin\bar{\beta}_i + \bar{c}_d \cos\bar{\beta}_i}{\left[\frac{\cos\bar{\beta}}{\cos(\bar{\beta}_i - \bar{\beta})}\right]^2} \frac{\bar{c}}{D} \frac{1 - x_h^4}{4} \tag{3b}$$

And finally

$$K_T = \varkappa_T \mathrm{B}^2 \left(\bar{c}_l \cos\bar{\beta}_i - \bar{c}_d \sin\bar{\beta}_i\right) \tag{4a}$$

$$K_Q = \varkappa_Q \mathrm{B}^2 \left(\bar{c}_l \sin\bar{\beta}_i + \bar{c}_d \cos\bar{\beta}_i\right) \tag{4b}$$

using the following abbreviations for convenience:

$$\varkappa_T = \frac{\pi^2 Z}{4} \frac{\bar{c}}{D} \frac{1 - x_h^3}{3} \tag{4c}$$

$$\varkappa_Q = \frac{\pi^2 Z}{8} \frac{\bar{c}}{D} \frac{1 - x_h^4}{4} \tag{4d}$$

$$\varkappa = \frac{\varkappa_Q}{\varkappa_T} = \frac{3}{8} \frac{1 - x_h^4}{1 - x_h^3} \tag{4e}$$

$$\mathrm{B} = \frac{\cos(\bar{\beta}_i - \bar{\beta})}{\cos\bar{\beta}} \tag{4f}$$

Furthermore the advance angle $\bar{\beta}$ is known for a given advance coefficient J:

$$\tan\bar{\beta} = \frac{v_0}{\omega \bar{r}} = \frac{J}{\pi \bar{x}} \tag{4g}$$

Let us recapitulate the dependencies of each variable on the advance coefficient J, the fractional radius $\bar{x}$ and the Reynolds number $\overline{\mathrm{Rn}}$ of the equivalent profile:

$\bar{c}$ $= \bar{c}(\bar{x})$

K_T $= K_T(J, \overline{\mathrm{Rn}})$

K_Q $= K_Q(J, \overline{\mathrm{Rn}})$

$\bar{c}_d$ $= \bar{c}_d(J, \overline{\mathrm{Rn}}, \bar{x})$

$\bar{c}_l$ $= \bar{c}_l(J, \bar{x})$

$\bar{\beta}$ $= \bar{\beta}(J, \bar{x})$

$\bar{\beta}_i$ $= \bar{\beta}_i(J, \bar{x})$

$\varkappa_T$ $= \varkappa_T(\bar{x})$

$\varkappa_Q$ $= \varkappa_Q(\bar{x})$

$\varkappa$ $= \mathrm{const}$

B $= \mathrm{B}(J, \bar{x})$

Strictly speaking the lift coefficient $\bar{c}_l$, the hydrodynamic inflow angle $\bar{\beta}_i$ and hence the factor B also depend on the Reynolds number, but this dependence is very weak as we will argue later.

3.2 Option 1 – Basic Profile Drag $\bar{c}_{d,0}$

For every propeller there is only one advance coefficient J_0, where the equivalent profile does not generate any lift. This is similar to the zero-lift angle of attack of an aerofoil. It is worth noting that this operating point does neither occur at the J-value where K_T or K_Q becomes zero but its position will be between those two points. We reference all values corresponding to J_0 with the subscript 0.

3.2.1 Determination of the Basic Profile Drag $\bar{c}_{d,0}$

Starting with the equations (4a+b) we set the lift coefficient $\bar{c}_l$ to 0:

$$K_{T,0} = \varkappa_T \mathrm{B}_0^2 \left(-\bar{c}_{d,0} \sin\bar{\beta}_{i,0}\right) \tag{5a}$$

$$K_{Q,0} = \varkappa_Q \mathrm{B}_0^2 \left(\bar{c}_{d,0} \cos\bar{\beta}_{i,0}\right) \tag{5b}$$

Isolating $\bar{c}_{d,0}$ from both equations and equalizing them, results in an equation for $\bar{\beta}_{i,0}$

$$-\frac{K_{T,0}}{\varkappa_T} \frac{1}{\sin\bar{\beta}_{i,0}} = \frac{K_{Q,0}}{\varkappa_Q} \frac{1}{\cos\bar{\beta}_{i,0}} \tag{6}$$

Which can be solved for $\bar{\beta}_{i,0}$:

$$\tan\bar{\beta}_{i,0} = -\frac{K_{T,0}}{\varkappa_T} \frac{\varkappa_Q}{K_{Q,0}} = -\varkappa \frac{K_{T,0}}{K_{Q,0}} \tag{7}$$

Unfortunately we still cannot determine $\bar{\beta}_{i,0}$ because we do not know at which value J_0 we have to evaluate the above equation. But if the equivalent profile does not produce any lift, it will not generate any induced velocities and hence the hydrodynamic inflow angle $\bar{\beta}_{i,0}$ becomes the advance angle $\bar{\beta}_i$ at J_0:

$$\tan\bar{\beta}_{i,0} = \tan\bar{\beta}_0 \tag{8a}$$

$$-\varkappa \frac{K_T(J_0)}{K_Q(J_0)} = \frac{J_0}{\pi \bar{x}} \tag{8b}$$

If we assume a value $\bar{x}$ for the radial position of the equivalent profile, we can numerically solve any of the following conditional equations for J_0.

$$\frac{J_0}{\pi \bar{x}} + \varkappa \frac{K_T(J_0)}{K_Q(J_0)} = 0 \tag{9a}$$

$$\frac{J_0}{\pi \bar{x}} K_Q(J_0) + \varkappa K_T(J_0) = 0 \tag{9b}$$

$$\frac{J_0^2}{2\pi^2 \bar{x}} + \varkappa \eta_O(J_0) = 0 \tag{9c}$$

A good choice for $\bar{x}$ might be either of the universally accepted values of 0.7 or 0.75.

With the value J_0 of the advance coefficient, where the lift coefficient $\bar{c}_l$ becomes zero, known, the hydrodynamic inflow angle $\bar{\beta}_{i,0}$ can be calculated with the help of equations (8b) and (7) and finally the basic profile drag $\bar{c}_{d,0}$ is known from evaluating any of the equations (5a) or (5b) with $K_{T,0}$ or $K_{Q,0}$ from the measured open-water data:

$$\bar{\beta}_{i,0} = \bar{\beta}_0 = \arctan\frac{J_0}{\pi \bar{x}} \tag{10}$$

$$\bar{c}_{d,0} = -\frac{K_{T,0}}{\varkappa_T \mathrm{B}_0^2 \sin\bar{\beta}_{i,0}} = \frac{K_{Q,0}}{\varkappa_Q \mathrm{B}_0^2 \cos\bar{\beta}_{i,0}} \tag{11}$$

3.2.2 Determination of the Hydrodynamic Inflow Angle $\bar{\beta}_i(J)$

Starting again from the two equations (4a+b)

$$\bar{c}_l \cos\bar{\beta}_i - \bar{c}_d \sin\bar{\beta}_i = \frac{K_T}{\varkappa_T \mathrm{B}^2} \tag{12a}$$

$$\bar{c}_l \sin\bar{\beta}_i + \bar{c}_d \cos\bar{\beta}_i = \frac{K_Q}{\varkappa_Q \mathrm{B}^2} \tag{12b}$$

(rearranged here for clarity) the lift coefficient $\bar{c}_l$ can be eliminated by multiplying (12a) with $\sin\beta_i$ and (12b) with $\cos\beta_i$ and subtracting the first from the second equation:

$$\bar{c}_d = \frac{1}{\mathrm{B}^2}\left(\frac{K_Q}{\varkappa_Q}\cos\bar{\beta}_i - \frac{K_T}{\varkappa_T}\sin\bar{\beta}_i\right) \tag{13}$$

The linearized profile theory states that the drag coefficient remains constant for small angles of attack α and is equal to the minimum drag coefficient which occurs at the operating point where the profile does not generate any lift (Abbott & von Doenhoff 1959). In the case of the equivalent profile this corresponds to the statement that the drag coefficient $\bar{c}_d(J)$ remains constant for all values of J and is equal to the basic profile drag $\bar{c}_{d,0}$ – as long as the angle of attack α is small:

$$\bar{c}_d(J) = \bar{c}_{d,0} \tag{14}$$

With this assumption equation (13) becomes the conditional equation for $\bar{\beta}_i(J)$ which can be solved numerically for any given J:

$$\frac{1}{\mathrm{B}^2|_J}\left(\frac{K_Q|_J}{\varkappa_Q}\cos\bar{\beta}_i|_J - \frac{K_T|_J}{\varkappa_T}\sin\bar{\beta}_i|_J\right) - \bar{c}_{d,0} = 0 \tag{15}$$

3.2.3 Determination of the Lift Coefficient $\bar{c}_l(J)$

Knowing the hydrodynamic inflow angle $\bar{\beta}_i$ from solving equation (15), the lift coefficient $\bar{c}_l$ can be calculated from equations (12a+b):

$$\begin{aligned}\bar{c}_l &= \frac{1}{\cos\bar{\beta}_i}\left(\frac{K_T}{\varkappa_T \mathrm{B}^2} + \bar{c}_{d,0}\sin\bar{\beta}_i\right)\\ &= \frac{1}{\sin\bar{\beta}_i}\left(\frac{K_Q}{\varkappa_Q \mathrm{B}^2} - \bar{c}_{d,0}\cos\bar{\beta}_i\right)\end{aligned} \tag{15}$$

3.3 Option 2 – Two Open-water Tests at Two Reynolds Numbers

We can use two open-water tests conducted at two different Reynolds numbers Rn_1 and Rn_2 to calculate the hydrodynamic inflow angle $\bar{\beta}_i(J)$, the lift and drag coefficients $\bar{c}_l(J)$ and $\bar{c}_d(J)$ and the added three-dimensional drag $\bar{c}_{d,3d}(J)$.

Starting with the equations (4a+b) we can eliminate the drag and lift coefficients $\bar{c}_d(J)$ and $\bar{c}_l(J)$ with the process described for the derivation of equation (13):

$$\bar{c}_l = \frac{1}{\mathrm{B}^2}\left(\frac{K_Q}{\varkappa_Q}\sin\bar{\beta}_i + \frac{K_T}{\varkappa_T}\cos\bar{\beta}_i\right) \tag{17a}$$

$$\bar{c}_d = \frac{1}{\mathrm{B}^2}\left(\frac{K_Q}{\varkappa_Q}\cos\bar{\beta}_i - \frac{K_T}{\varkappa_T}\sin\bar{\beta}_i\right) \tag{17b}$$

The theory of aerofoils states that the lift coefficient $\bar{c}_l$ does not change with the Reynolds number (Abbott & von Doenhoff 1959). We can (reasonably) assume that if the lift does not change, the induced velocities will not change either, hence the hydrodynamic inflow angle $\bar{\beta}_i$ does not change with the Reynolds number for any given value of J:

$$\bar{c}_{l,1}(J) = \bar{c}_{l,2}(J) = \bar{c}_l(J) \tag{18a}$$

$$\bar{\beta}_{l,1}(J) = \bar{\beta}_{l,2}(J) = \bar{\beta}_i(J) \tag{18b}$$

where the subscripts 1 and 2 denote the values corresponding to each of the two Reynolds numbers Rn_1 and Rn_2.

By equalizing the equation (17a) evaluated at both Reynolds numbers, we get an analytical equation for the hydrodynamic inflow angle $\bar{\beta}_i(J)$:

$$\begin{aligned}&\frac{1}{\mathrm{B}^2}\left(\frac{K_{Q,1}}{\varkappa_Q}\sin\bar{\beta}_i + \frac{K_{T,1}}{\varkappa_T}\cos\bar{\beta}_i\right)\\ &\quad = \frac{1}{\mathrm{B}^2}\left(\frac{K_{Q,2}}{\varkappa_Q}\sin\bar{\beta}_i + \frac{K_{T,2}}{\varkappa_T}\cos\bar{\beta}_i\right)\end{aligned} \tag{19a}$$

$$\tan\bar{\beta}_i = -\varkappa\frac{K_{T,1} - K_{T,2}}{K_{Q,1} - K_{Q,2}} = -\varkappa\frac{\Delta K_T}{\Delta K_Q} \tag{19b}$$

Substituting the now known value $\bar{\beta}_i$ into equations (17a+b) will yield the same lift coefficient for both Reynolds numbers but two different drag coefficients $\bar{c}_{d,1}(J)$ and $\bar{c}_{d,2}(J)$. An interesting observation is that both the hydrodynamic inflow angle and these coefficients are independent of the fractional radius $\bar{x}$ of the equivalent profile.

3.4 Option 3 – Determination of the Hydrodynamic Inflow Angle $\bar{\beta}_i$ from Just One Open-water Test

As seen above in equation (19b) the hydrodynamic inflow angle $\bar{\beta}_i$ over the range of the advance coefficient J can be calculated from the K_T and K_Q curves. In the following section a formal way do derive this hydrodynamic inflow angle from a single set of thrust and torque curves will be presented.

Starting with equation (17a), we reshape it to (and show their dependencies)

$$\begin{aligned}&\mathrm{B}^2(J,\overline{\mathrm{Rn}})\bar{c}_l(J,\overline{\mathrm{Rn}})\\ &\quad = \frac{K_Q(J,\overline{\mathrm{Rn}})}{\varkappa_Q}\sin\bar{\beta}_i(J,\overline{\mathrm{Rn}})\\ &\quad + \frac{K_T(J,\overline{\mathrm{Rn}})}{\varkappa_T}\cos\bar{\beta}_i(J,\overline{\mathrm{Rn}})\end{aligned} \tag{20a}$$

Usually this equation is looked at with the Reynolds number $\overline{\mathrm{Rn}}$ fixed resulting in the well-known open-water curves $K_T(J)|_{\overline{\mathrm{Rn}}}$, $K_Q(J)\big|_{\overline{\mathrm{Rn}}}$ and $\eta_o(J)|_{\overline{\mathrm{Rn}}}$. If the same propeller were tested at different Reynolds numbers, the three-dimensional surfaces $K_T(J,\overline{\mathrm{Rn}})$ and $K_Q(J,\overline{\mathrm{Rn}})$ can be constructed. Cutting these surfaces at constant J-values results in the open-water curves $K_T(\overline{\mathrm{Rn}})|_J$ and $K_Q(\overline{\mathrm{Rn}})\big|_J$ depending on the Reynolds number. Omitting $|_J$, which indicates that the J-value is fixed, for clarity, equation (20a) is written for fixed values of J as

$$\mathrm{B}^2(\overline{\mathrm{Rn}})\overline{c}_l(\overline{\mathrm{Rn}}) = \frac{K_Q(\overline{\mathrm{Rn}})}{\varkappa_Q}\sin\overline{\beta}_i(\overline{\mathrm{Rn}}) + \frac{K_T(\overline{\mathrm{Rn}})}{\varkappa_T}\cos\overline{\beta}_i(\overline{\mathrm{Rn}}) \tag{20b}$$

We again assume that the hydrodynamic inflow angle $\overline{\beta}_i$ and the lift coefficient $\overline{c}_l$ do not change with the Reynolds number, hence the coefficient B and the lift coefficient stay constant for a fixed J-value. This assumption will certainly hold true as long as no flow separation occurs:

$$B^2\bar{c}_l = K_Q\frac{\sin\overline{\beta}_i}{\varkappa_Q} + K_T\frac{\cos\overline{\beta}_i}{\varkappa_T} \tag{21a}$$

We differentiate with respect to $\overline{\mathrm{Rn}}$

$$0 = \frac{\mathrm{d}K_Q}{\mathrm{d}\overline{\mathrm{Rn}}}\frac{\sin\overline{\beta}_i}{\varkappa_Q} + \frac{\mathrm{d}K_T}{\mathrm{d}\overline{\mathrm{Rn}}}\frac{\cos\overline{\beta}_i}{\varkappa_T} \tag{21d}$$

and multiply by $\mathrm{d}\overline{\mathrm{Rn}}$

$$0 = \mathrm{d}K_Q\frac{\sin\overline{\beta}_i}{\varkappa_Q} + \mathrm{d}K_T\frac{\cos\overline{\beta}_i}{\varkappa_T} \tag{21d}$$

Now we can isolate the hydrodynamic inflow angle $\bar{\beta}_i$:

$$\tan\overline{\beta}_i = -\frac{\varkappa_Q}{\varkappa_T}\frac{\mathrm{d}K_T}{dK_Q} = -\varkappa\frac{\mathrm{d}K_T}{dK_Q} \tag{22a}$$

or when using thrust and torque figures:

$$\tan\overline{\beta}_i = -\varkappa\frac{D\mathrm{d}T}{\mathrm{d}Q} \tag{22b}$$

These equations determine the hydrodynamic inflow angle $\overline{\beta}_i$ over the whole range of the advance coefficient J just from the slope of the $K_T(K_Q)$-curve. This relationship is strictly speaking only valid if the thrust and torque were measured at a constant Reynolds number (see appendix "A.2 Open-water Tests at Constant Reynolds number" how this can be achieved). Now the equation (22a) can be rewritten as

$$\tan\overline{\beta}_i = -\varkappa\frac{\frac{\partial K_T}{\partial J}}{\frac{\partial K_Q}{\partial J}} \tag{23}$$

which facilitates the calculation, if the K_T and K_Q curves are given in their polynomial form.

The drag and lift coefficients can now be calculated from equations (17a+b). They do not depend on the location $\overline{x}$ of the equivalent profile, neither does the hydrodynamic inflow angle $\bar{\beta}_i$.

4 FULL SCALE EXTRAPOLATION

Any of the three analysis presented above yields the values of the lift and drag coefficients $\overline{c}_l$ and $\overline{c}_d$ and the hydrodynamic inflow angle $\bar{\beta}_i$ for a particular open-water test (set of equations: [(17), (12), (16)], [(18b), (18a), (20b)], [(18b), (18a), (22a or b) (23)]). These values can be scaled separately using the theory of aerofoil sections and the corresponding experimental results.

4.1 Scaling the lift coefficient $\overline{c}_l$

Using results from the profile theory, it can be assumed that the lift coefficient $\overline{c}_l$ remains constant when the Reynolds number changes.

Sometimes it is claimed that this assumption does not generally hold for all cases. There is no reason why the lift coefficient cannot be scaled with any appropriate method already existing or becoming available in the future.

4.2 Scaling the hydrodynamic inflow angle $\overline{\beta}_i$

If the lift coefficient and hence the lift do not change, the induced velocities will not change either. That is equivalent to the statement that the hydrodynamic inflow angle $\bar{\beta}_i$ does not change with changes in the Reynolds number. If the lift coefficient $\overline{c}_l$ were to be scaled, it is to be assumed that the influence on $\bar{\beta}_i$ is negligibly small and hence can be neglected.

That leaves us with the drag coefficient $\overline{c}_d$ to be scaled.

4.3 Scaling the drag coefficient $\overline{c}_d$

The drag coefficient of a section can be split into a contribution of the friction $\overline{c}_f$ and the section form drag $\overline{c}_{d,2d}$ (ITTC 1999)(Kuiper 1992)(Abbott & von Doenhoff 1959):

$$\overline{c}_d = 2\overline{c}_f \cdot \overline{c}_{d,2d} \tag{24}$$

Analyzing the data available to the author using the empirical formulae for the section form drag (Abbott & von Doenhoff (1959) give the form drag as stated here, but often the last term $60(\overline{t}/\overline{c})^4$ is not taken into account, because its contribution is very small (ITTC 1999)(Kuiper1992))

$$\overline{c}_{d,2d} = 1 + 2\frac{\overline{t}}{\overline{c}} + 60\left(\frac{\overline{t}}{\overline{c}}\right)^4 \tag{25}$$

and the ITTC 78 friction line (ITTC 1999)

$$\overline{c}_f = \frac{0.04}{\overline{\mathrm{Rn}}^{1/6}} - \frac{5}{\overline{\mathrm{Rn}}^{2/3}} \tag{25}$$

shows that the drag coefficients calculated with equations (17b) and (24) differ substantially. Kuiper (1992) mentions in his book that van Oossanens introduces a drag coefficient ${}^{\Sigma}\overline{c}_{d,3d}$ to account for "three-dimensional effects", which is added to the profile drag:

$$\overline{c}_d = 2\overline{c}_f \cdot \overline{c}_{d,2d} + {}^{\Sigma}\overline{c}_{d,3d} \tag{27}$$

According to these authors this three-dimensional added drag coefficient ${}^{\Sigma}\overline{c}_{d,3d}$ does not change with the Reynolds number.

In the author's opinion a proportional factor ${}^{\Pi}\overline{c}_{d,3d}$ is more suitable and would fit into the concept of the (two-dimensional) section form drag $\overline{c}_{d,2d}$:

$$\overline{c}_d = 2\overline{c}_f \cdot \overline{c}_{d,2d} \cdot {}^{\Pi}\overline{c}_{d,3d} \tag{28}$$

If no flow separation occurs, the section form drag $\overline{c}_{d,2d}$ only depends on geometrical features but neither on the Reynolds number nor on the advance coefficient, hence it is constant. The factor ${}^{\Pi}\overline{c}_{d,3d}$ accounts for the three-dimensional effects of the flow around the propeller and hence depends only on the advance coefficient. (Strictly speaking there will be an influence of the Reynolds number as well, since the thickness of the boundary layer changes and hence the three-dimensional flow around the propeller. For the moment we deliberately disregard this small effect.) The friction drag coefficient $\overline{c}_f$ depends strongly on the Reynolds number:

$$\overline{c}_d(J, \overline{\mathrm{Rn}}) = 2\overline{c}_f(\overline{\mathrm{Rn}}) \cdot \overline{c}_{d,2d} \cdot {}^{\Pi}\overline{c}_{d,3d}(J) \tag{28}$$

If the friction coefficient $\overline{c}_f$ were known, the three-dimensional drag $\overline{c}_{\mathrm{d,3d}}$ can be calculated from the model test. Finally the drag coefficient $\overline{c}_d$ for any scale can be reassembled with the friction coefficient $\overline{c}_f$ for the selected Reynolds number, e.g. full scale propeller or self-propulsion test.

4.4 Scaling the friction drag coefficient $\overline{c}_f$

The scaling of the friction drag with the Reynolds number is a matter of ongoing discussion. In the scope of this paper only some observations or suggestions should be made.

The difficulty of scaling propellers stems from the fact that the Reynolds numbers reached during open-water tests falls into the transitional region where the flow over the blades is not fully turbulent yet.

The traditional way to scale the friction drag coefficient $\overline{c}_f$ is to use friction lines derived from experiments. One line which is universally used in the field of naval architecture is the ITTC 1978 friction line (ITTC 1999). The note made in section 2.2 should always be kept in mind.

Another friction line often used in fluid dynamics is the Schlichting line (Schlichting & Gersten (2006)):

$$c_f = \frac{0.031}{\mathrm{Rn}^{\frac{1}{7}}} - \frac{\gamma}{\mathrm{Rn}} \tag{29}$$

where the value of the factor γ depends on the local Reynolds number where the transition from laminar to turbulent flow occurs.

These friction lines are applied to the equivalent profile.

A second approach is shown by Streckwall et al (2013). They integrate the local laminar and turbulent friction coefficients $c_{f,x,lam}$ and $c_{f,x,turb}$ along the section using two different formulations for the laminar and turbulent region (Hoerner 1965). The transition point is calculated by CFD methods.

$$c_{f,x,lam} = \frac{0.664}{\mathrm{Rn}_x^{0.5}} \tag{30a}$$

$$c_{f,x,turb} = \frac{0.0592}{\mathrm{Rn}_x^{0.2}} \tag{30b}$$

where Rn_x is the Reynolds number with respect to the distance from the leading edge of the profile.

Some suggestions to improve the calculation of the friction drag are:

- Using two open-water tests at different Reynolds numbers would result in two drag coefficients for the same J-value. If the friction line used has a second parameter beside the Reynolds number (like the Schlichting friction line), evaluating equation (28) for both Reynolds numbers results in two equations for the unknowns ${}^{\Pi}\overline{c}_{d,3d}$ and this parameter, which can be readily solved.
- Instead of evaluating the friction line just for the equivalent profile, the friction drag can be integrated over the propeller blade as done by Streckwall et al (2013).
- If the location of the transition from laminar to turbulent flow were known, the local friction drag (30a+b) can be integrated over the blade using the actual transition point. This transition point could be established during the open-water test with a paint test. This approach would honor the actual section shapes.
- The friction drag can be calculated by solving the boundary layer equations for the actual section used with the help of computer programs such as XFOIL (Drela 2013) or JavaFoil (Hepperle 2006). This can be done for the equivalent section or – preferably – for each section with the subsequent integration over the blade.
- Since the laminar drag is well known, the propeller could be tested strictly with laminar flow over it. This removes the uncertainty of the transitional region. If

the flow remains attached over the whole bladed needs to be established.

5. EXEMPLARY RESULTS

5.1 Scaling of open-water experiments

A NPT propeller designed by Stone Marine Propulsion and a conventional propeller of the Wageningen B type were tested at three different Reynolds numbers at the model basin of SSPA in Gothenburg (table 1 and figures 1 and 6). All six open-water curves were scaled according to the ITTC 1978 (figures 2 and 7), the Lerbs-Meyne (figures 3 and 8), the strip method (figures 4 and 9) and the proposed new method, option 3 (figures 5 and 10). The new method uses the ITTC friction line to calculate $\overline{c}_f$.

Table 1: Main particulars of the propellers analyzed.

	Conventional	NPT	
D	7.3	6.8	m
P/D	0.673	0.902	–
$c_{0.7}$	1.9563	1.799	m
A_e/A_0	0.53	0.460	–
Z	4	4	–
λ	33.1818	27.143	–
Type	Wageningen B	New profile technology	

It is noticeable that the lowest Reynolds numbers of $2.5 \cdot 10^5$ and $3.5 \cdot 10^5$ is too low for all methods. The first three methods work reasonably well for the conventional propeller, whereas the scaled values for the NPT propeller shows a noticeable gap between the extrapolated efficiencies.

Applying the new method to the conventional propeller moves the efficiency curves scaled from the two higher Reynolds numbers on top of each other. For the NPT propeller the difference between these efficiency curves decreases noticeably.

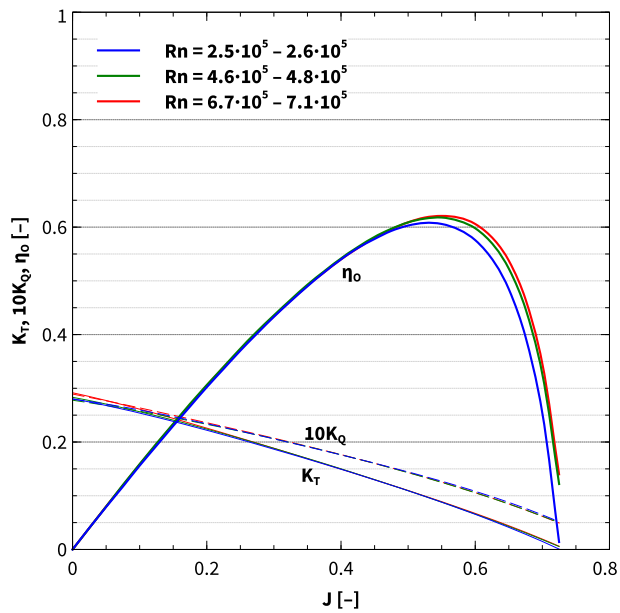

Figure 1: Open-water characteristics of the conventional propeller, measured values.

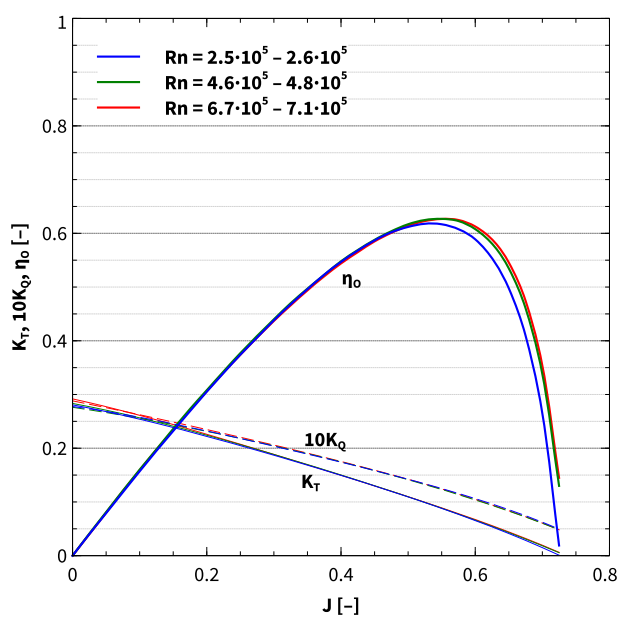

Figure 2: Open-water characteristics of the conventional propeller, scaled according to the ITTC 1978 method.

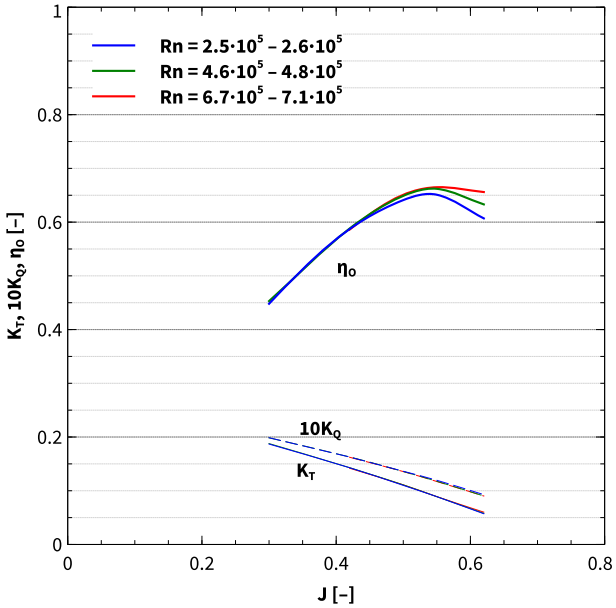

Figure 3: Open-water characteristics of the conventional propeller, scaled with the Lerbs-Meyne method. (Courtesy of H. Streckwall.)

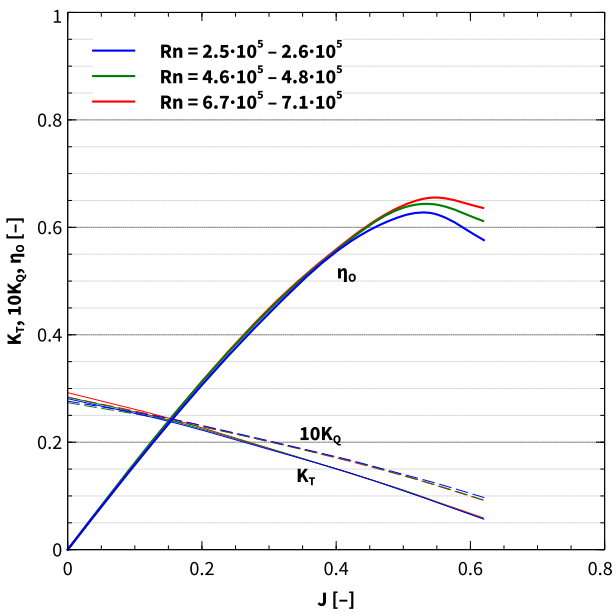

Figure 4: Open-water characteristics of the conventional propeller, scaled with the strip method. (Courtesy of H. Streckwall.)

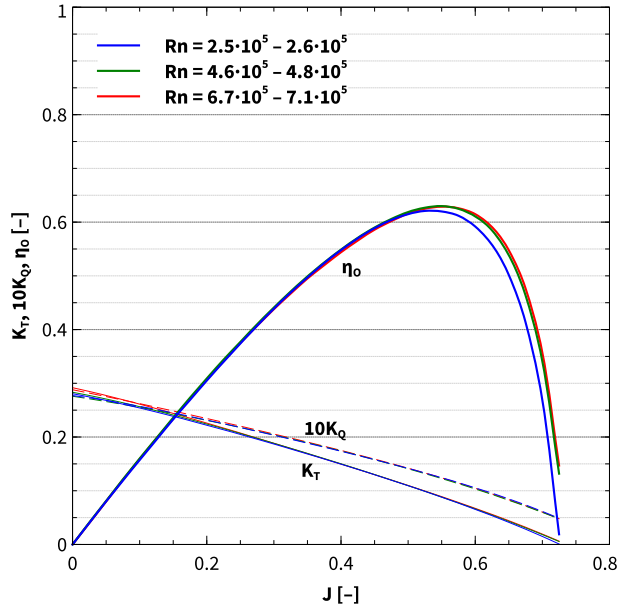

Figure 5: Open-water characteristics of the conventional propeller, scaled with the new method, option 3.

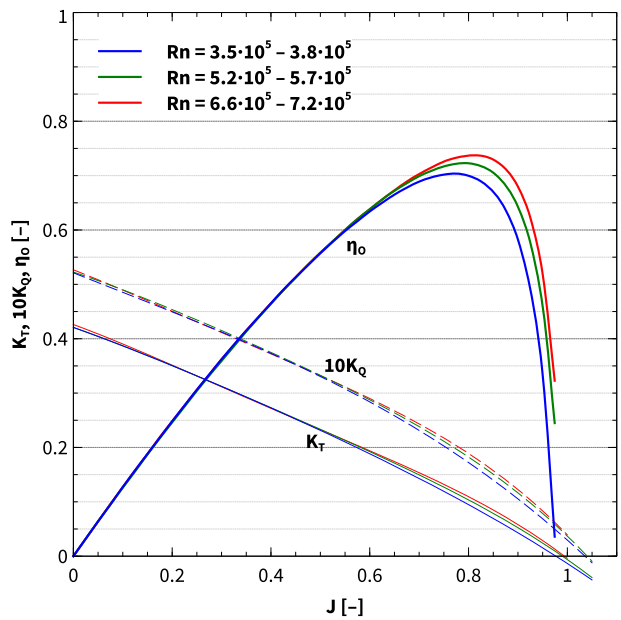

Figure 6: Open-water characteristics of the NPT propeller, measured values.

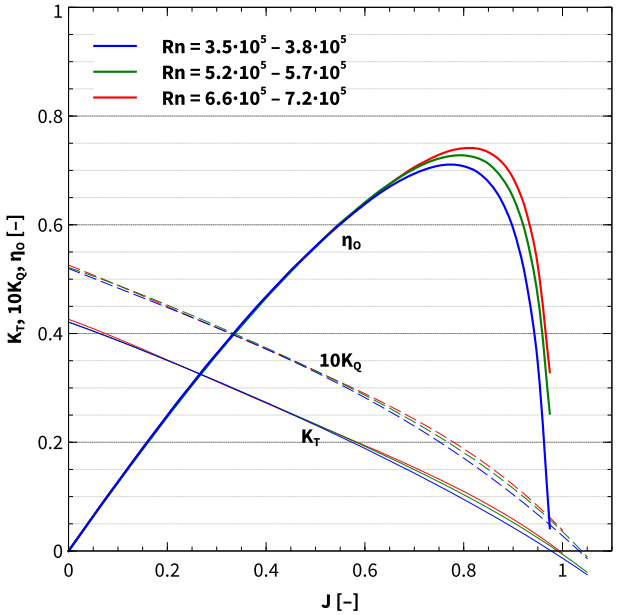

Figure 7: Open-water characteristics of the NPT propeller, scaled according to the ITTC 1978 method.

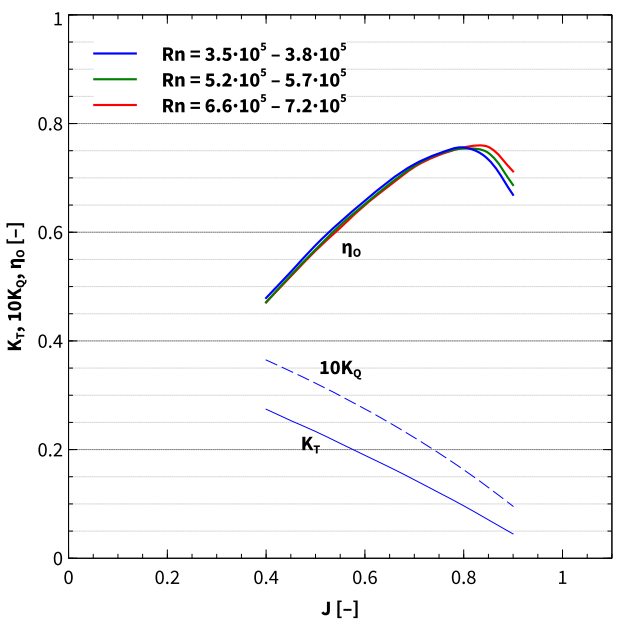

Figure 8: Open-water characteristics of the NPT propeller, scaled with the Lerbs-Meyne method. (Courtesy of H. Streckwall.)

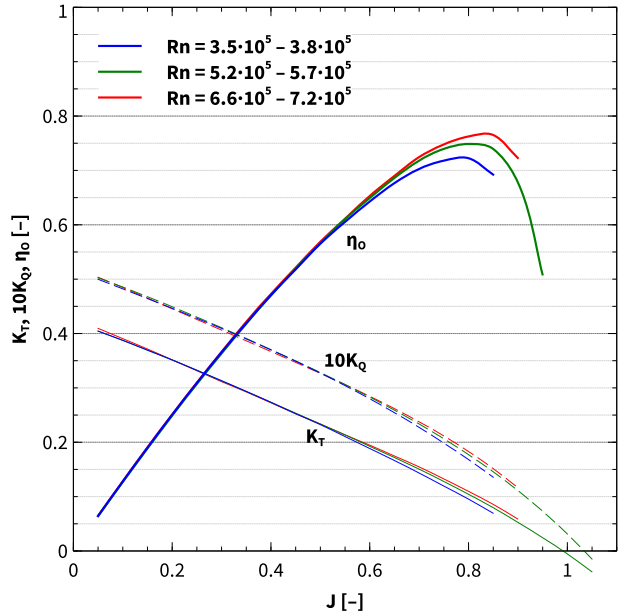

Figure 9: Open-water characteristics of the NPT propeller, scaled with the strip method. (Courtesy of H. Streckwall.)

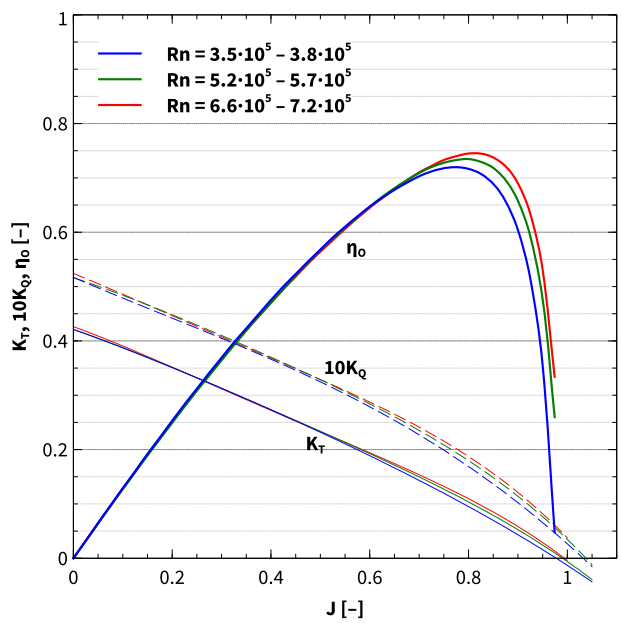

Figure 10: Open-water characteristics of the NPT propeller, scaled with the new method, option 3.

5.2 Effects on power prediction

As a case study to show the effects of the new scaling procedure on the power prediction, a 6700 PCTC car carrier was chosen. This is the vessel the NPT propeller used in the section 5.1 was designed for (see Table 1 for the main particulars of the propeller).

The self-propulsion test was analyzed with the three different open-water curves using the ITTC 1978 performance prediction method. Subsequently the power prediction was calculated using the open-water characteristics from the same open-water curve as used for the analysis but extrapolated according to the ITTC 1978 and the new method from section 3.4. The predicted power demand curves are shown in figures 11 and 12. These figures show that the curves for the new method are closer when compared to the ITTC curves. To investigate this effect the differences between the high and low range Reynolds number prediction to the mid range Reynolds number prediction have been calculated for each of the two extrapolation methods. The results are shown in figure 13. It can be seen that for the ITTC method the differences increase with the ship speed whereas the differences for the new method cross each other roughly at the design speed.

Further it can be noticed that the differences for the new method are considerably smaller for the whole range of the ship speed. The differences in the power prediction for the ITTC and the new method can be seen in figure 14. The new method predicts a higher ship speed for the same power which is in accordance with the experience of the manufacturer of the NPT propeller where their propellers regularly achieve higher speeds during sea trials than predicted.

Some model basins claim that the self-propulsion tests should be analyzed with the open-water characteristics at the Reynolds number of the model propeller experienced during the self-propulsion tests. In the current test case the rate of revolution for the measured open-water curve at the low Reynolds number range is close to the shaft speed during the self-propulsion test, hence it was used to analyze the self-propulsion test. For the power prediction the values from the extrapolated open-water curves were used. The results are shown in figure 15 for the ITTC scaling method. Surprisingly the difference between these two power predictions is bigger than the difference between the power predictions based on the open-water characteristics with the same Reynolds number used for the analysis and the prediction (see figure 16). This behavior can be observed for the ITTC and the new extrapolation method. The reason for this discrepancy to the theory predicting a smaller difference is not known.

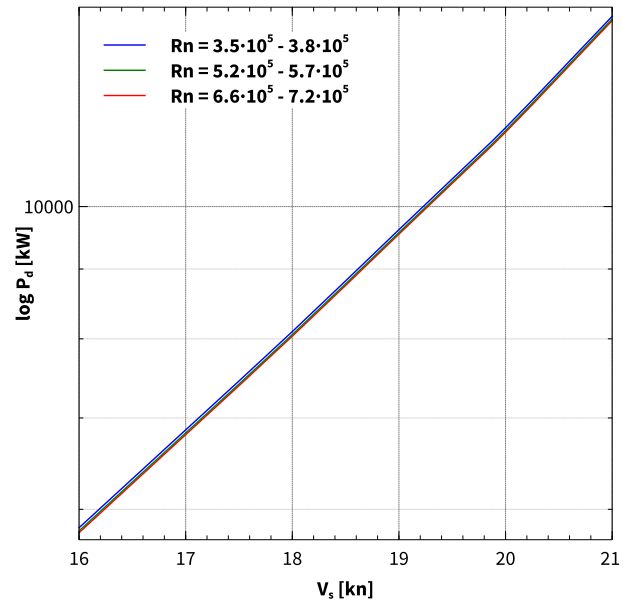

Figure 11: Power prediction for the case study based on open-water characteristics scaled according to the ITTC 1978 method.

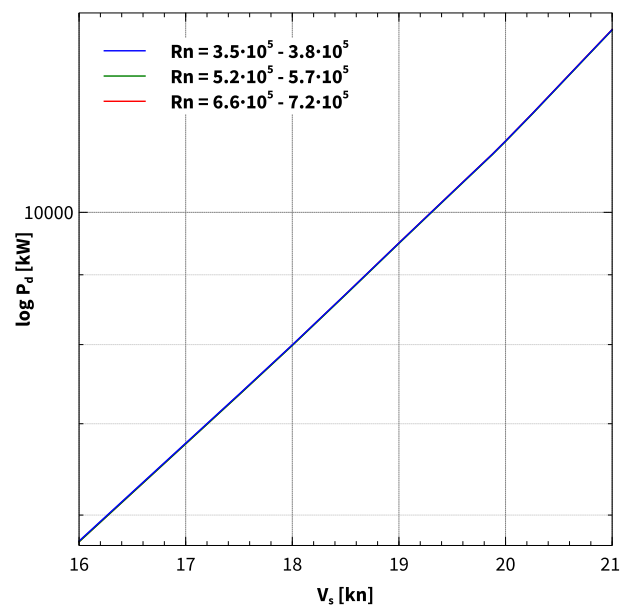

Figure 12: Power prediction for the case study based on open-water characteristics scaled with the new method, option 3.

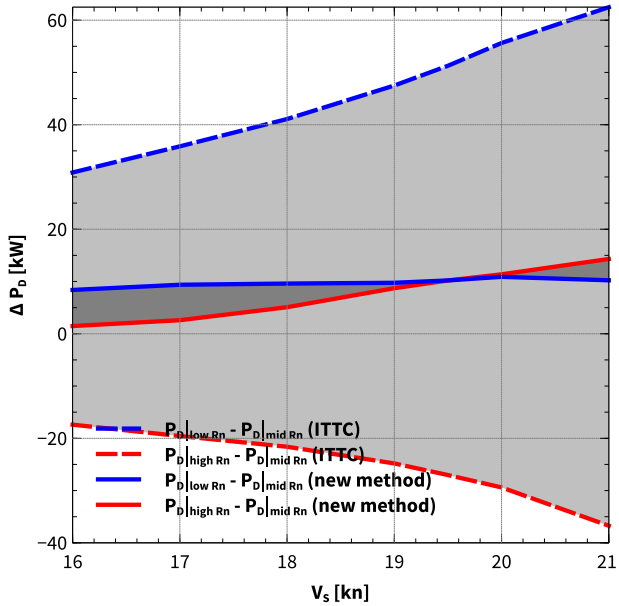

Figure 13: Differences between the power predictions for the case study based on open-water characteristics scaled according to the ITTC 1978 and the new (option 3) method. Shown are the differences to predictions based on the mid range Reynolds number.

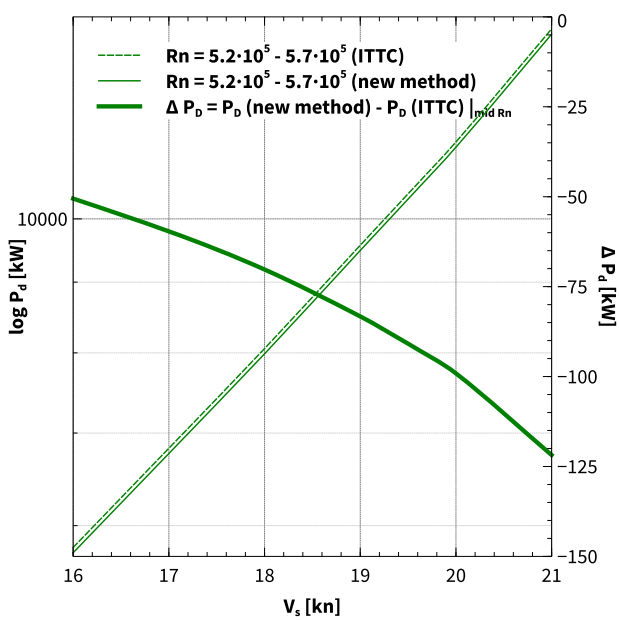

Figure 14: Power predictions and their difference for the case study based on open-water characteristics scaled according to the ITTC 1978 and the new method.

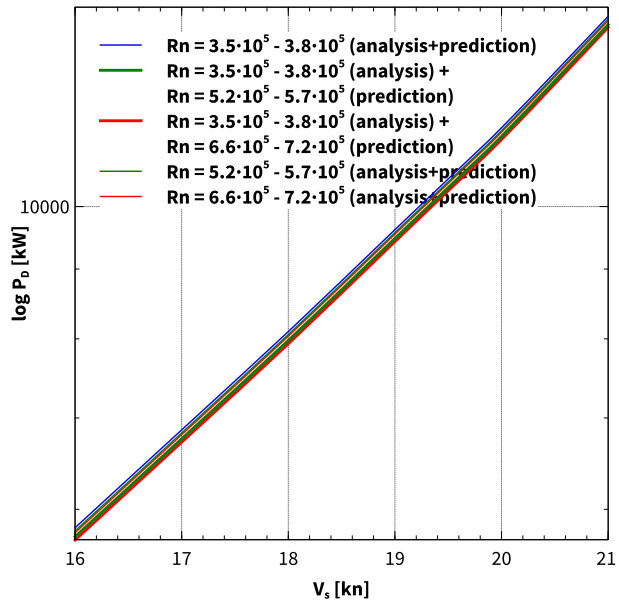

Figure 15: Power predictions based on the analysis with the open-water characteristics at the low Reynolds number range for the case study. The thin lines are those of figure 11 and are shown for reference. The scaling is done according to the ITTC 1978.

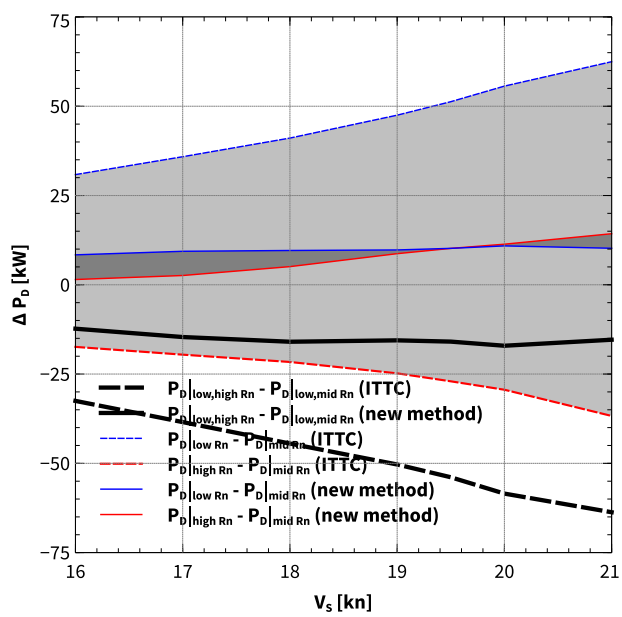

Figure 16: Differences between the power predictions for the case study based on the analysis with the open-water characteristics at the low Reynolds number range. The blue and red graphs are those from figure 13 and are shown for reference.

6. CONCLUSIONS

A new method to extrapolate open-water performance data was presented. It makes use of the concept of the equivalent profile. It is entirely independent of the propeller geometry or the blade loading and works for all propellers which do not experience flow separation. By calculating the hydrodynamic inflow angle from just one set of open-water curves, it is able to align the drag and friction forces to the actual inflow as the theory of wings suggests.

This new method has the potential to replace the existing methods as shown in the exemplary results.

This new method should be applied to as many performance predictions as possible and compared with the trials data to validate its suitability. This can only be done by a model basin which has the extensive data base to make this comparison reliable.

It was also shown that the ITTC 1978 recommendation for a minimum Reynolds number of $2{\cdot}10^5$ might be too low and it should be considered to be raised.

ACKNOWLEDGEMENTS

This research was made possible due to Stone Marine Propulsion Ltd positive attitude towards a new scaling method. A special thanks goes to Heinrich Streckwall from HSVA who kindly offered to calculate the open-water according to the Lerbs-Meyne- and the new strip method.

REFERENCES

Abbott, I. H. & von Doenhoff, A. E. (1959). 'Theory of Wing Sections'. Dover Publications, Inc, New York, USA.

Drela, M (2013). 'XFOIL. Subsonic Airfoil Development System'. http://web.mit.edu/drela/Public/web/xfoil/.

Hepperle, M (2006). 'JavaFoil – Analysis of Airfoils'. http://www.mh-aerotools.de/airfoils/javafoil.htm.

Hoerner, S (1965). 'Fluid Dynamic Drag: Practical Information on Aerodynamic Drag and Hydrodynamic Resistance'. Hoerner Fluid Dynamics.

ITTC (1999). '1978 ITTC Performance Prediction Method'. ITTC – Recommended Procedures and Guidelines, 7.5 – 02 – 03 – 01.4.

Kramer, K. N. (1939). 'The Induced Efficiency of Optimum Propellers Having a Finite Number of Blades', NACA **TM 884**.

Kuiper, G. (1992). 'The Wageningen Propeller Series'. MARIN Publication 92-001, Wageningen, The Netherlands.

Meyne, K. (1968). 'Experimentelle und theoretische Betrachtungen zum Maßstabseffekt bei Modellpropeller-Untersuchungen'. Schiffstechnik, Vol 15.

Schlichting, H. & Gersten, K (2006). 'Grenzschicht-Theorie'. Springer, Berlin, Heidelberg, New York.

Streckwall, H., Greitsch, L., Müller, J., Scharf, M. & Bugalski, T. (2013). 'Development of a Strip Method Proposed to Serve as a New Standard for Propeller Performance Scaling', Ship Technology Research **60**, No. 2, p. 58-60.

APPENDIX

A.1 Alternative Formulation of the Equivalent Profile

In section "3.1 Equivalent Profile" the blade was replaced by a single profile where all variables depending on the fractional radius x were considered constant. Alternatively only unknown values could be replaced by their constant counterpart from the equivalent profile.

It can be noticed that the difference $\beta_i - \beta$ is small, hence $\cos(\beta_i - \beta)$ is approximately 1. The equations (1a+b) become

$$K_T = \frac{\pi^2 Z}{4}\int_{x_h}^{1} \frac{c_l(x)\cos\beta_i(x) - c_d(x)\sin\beta_i(x)}{\cos^2\beta(x)}\frac{c(x)}{D}x^2\mathrm{d}x \tag{A1a}$$

$$K_Q = \frac{\pi^2 Z}{8}\int_{x_h}^{1} \frac{c_l(x)\sin\beta_i(x) + c_d(x)\cos\beta_i(x)}{\cos^2\beta(x)}\frac{c(x)}{D}x^3\mathrm{d}x \tag{A1a}$$

Here the lift and drag coefficients c_l and c_d and the hydrodynamic inflow angle β_i are unknown and will be replaced by the values of the equivalent profile such that the K_T and K_Q values do not change. Now these values can be written outside the integral:

$$K_T = \frac{\pi^2 Z}{4}\left(\overline{c}_l\cos\overline{\beta}_i - \overline{c}_d\sin\overline{\beta}_i\right)\int_{x_h}^{1} \frac{1}{\cos^2\beta(x)}\frac{c(x)}{D}x^2\mathrm{d}x \tag{A2a}$$

$$K_Q = \frac{\pi^2 Z}{8}\left(\overline{c}_l\sin\overline{\beta}_i + \overline{c}_d\cos\overline{\beta}_i\right)\int_{x_h}^{1} \frac{1}{\cos^2\beta(x)}\frac{c(x)}{D}x^3\mathrm{d}x \tag{A2b}$$

Introducing abbreviations as before:

$$K_T = \gamma_T\left(\overline{c}_l\cos\overline{\beta}_i - \overline{c}_d\sin\overline{\beta}_i\right) \tag{A3a}$$

$$K_Q = \gamma_Q\left(\overline{c}_l\sin\overline{\beta}_i + \overline{c}_d\cos\overline{\beta}_i\right) \tag{A3b}$$

with

$$\gamma_T = \frac{\pi^2 Z}{4}\int_{x_h}^{1} \frac{1}{\cos^2\beta(x)}\frac{c(x)}{D}x^2\mathrm{d}x \tag{A4a}$$

$$\gamma_Q = \frac{\pi^2 Z}{8}\int_{x_h}^{1} \frac{1}{\cos^2\beta(x)}\frac{c(x)}{D}x^3\mathrm{d}x \tag{A4b}$$

$$\gamma = \frac{\gamma_Q}{\gamma_T} = \frac{1}{2}\frac{\int_{x_h}^{1} \frac{1}{\cos^2\beta(x)} \frac{c(x)}{D} x^3 \mathrm{d}x}{\int_{x_h}^{1} \frac{1}{\cos^2\beta(x)} \frac{c(x)}{D} x^2 \mathrm{d}x} \tag{A4c}$$

All equations developed for the equivalent profile can be used by replacing $\varkappa_T \mathrm{B}^2$, $\varkappa_q \mathrm{B}^2$ and $\varkappa$ with γ_T, γ_Q and γ, respectively.

A.2 Open-water Tests at Constant Reynolds Number

Traditionally the model basins keep the propeller revolutions constant and change the carriage speed when conducting open-water tests. This results in a range of Reynolds numbers. It would be perfectly feasible to reduce the shaft revolutions whenever the carriage speed increases to keep the Reynolds number constant.

For any given change ΔJ of the advance coefficient J, the changes Δn and Δv_0 in propeller revolutions and carriage speed, respectively, are:

$$n + \Delta n = n \frac{\sqrt{J^2 + (\pi\overline{x})^2}}{\sqrt{(J + \Delta J)^2 + (\pi\overline{x})^2}} \tag{A5a}$$

$$v_0 + \Delta v_0 = v_0 \frac{\sqrt{1 + \left(\frac{\pi\overline{x}}{J}\right)^2}}{\sqrt{1 + \left(\frac{\pi\overline{x}}{J+\Delta J}\right)^2}} \tag{A5b}$$